Int. J. Heat Mass Transfer. Vol. 5, pp. 941–954. Pergamon Press 1962. Printed in Great Britain.

FILM CONDENSATION IN A FORCED-CONVECTION BOUNDARY-LAYER FLOW

J. C. Y. KOH*

The Boeing Company, Seattle, Washington

(*Received* 3 *November* 1961 *and in revised form* 30 *March* 1962)

Abstract—Laminar film condensation of a saturated vapor in forced flow over a flat plate is analysed. The problem is formulated as an exact boundary-layer solution. From numerical solutions of the governing equations, it is found that the energy transfer by convection is negligibly small for low Prandtl number liquids (liquid metals) but quite important for high Prandtl number liquids. The condensation rate, skin friction and heat transfer are presented in graphs as a function of $c_p\Delta T/Prh_{fg}$ with $[(\rho\mu)_L/(\rho\mu)_v]^{1/2}$ and Pr as parameters.

NOMENCLATURE

c_f, friction coefficient, equation (29);
c_p, specific heat at constant pressure;
f, dimensionless liquid stream function, equation (12);
F, dimensionless vapor stream function, equation (12);
h, local heat-transfer coefficient, equation (32);
k, thermal conductivity;
$\dot{m}$, mass flow at interface (mass condensed per unit time per unit area);
Nu_x, local Nusselt number, equation (31);
Pr, liquid Prandtl number, $(\mu c_p/k)_L$;
q, local heat-transfer rate per unit area;
R, equation (14);
Re_x, Reynolds number, $u_\infty x/\nu_L$;
T, static temperature;
ΔT, $T_s - T_w$;
u, velocity component in x-direction;
v, velocity component in y-direction;
x, co-ordinate measuring distance along plate from leading edge;
y, co-ordinate measuring distance normal to the plate;
η, similarity variable, equation (11);
η_δ, dimensionless liquid film thickness;
θ, dimensionless temperature, $(T - T_s)/(T_w - T_s)$;
μ, absolute viscosity;
ν, kinematic viscosity;
ρ, density;
ψ, stream function.

Subscripts

B, Blasius;
i, liquid vapor interface;
∞, free stream;
L, liquid;
v, vapor;
w, wall;
δ, at the liquid vapor interface;
L, i, liquid at the interface;
v, i, vapor at the interface.

Superscripts

$\bar{}$, average;
$'$, differentiation with respect to η_L or η_v.

I. INTRODUCTION

CONDENSATION heat transfer has been a subject of study for many years. Heretofore, research on this subject has been focused on natural convection where the fluid motion is generated by gravity forces [1–4]. Recent engineering developments, such as aerospace planes, nuclear reactors, etc., require the knowledge of fluid mechanics and heat transfer in the condensation processes under forced flow. Accordingly, a research program was initiated to study the condensation processes for flow over a flat plate. Simultaneously, Cess [5] treated the similar problem

* Research Specialist.

by neglecting inertia forces and energy transfer by convection in the governing liquid-flow equations. Chung [6] analysed the film-condensation processes by neglecting the vapor tangential velocity at the interface. The present paper reports the exact solutions of the differential equations for laminar-film condensation in forced flow over a flat plate.

II. ANALYSIS

Physical model and co-ordinate systems

Figure 1 shows a sketch of the physical model and co-ordinate system used for the present study. A stream of vapor at a velocity u_∞ is flowing over the plate. The vapor is at a saturation temperature T_s. The plate surface temperature T_w is lower than T_s and hence condensation takes place. It is assumed that, in steady state, there exists a smooth liquid film adjacent to the plate surface. At the plate surface, the liquid velocity is zero. Away from the surface, the liquid moves under the influence of drag forces. The vapor velocity approaches the free stream velocity at some distances from the plate. Therefore, there exist both liquid and vapor boundary layers simultaneously. Since the liquid flow is due to the drag force exerted by the vapor, and the presence of the liquid motion in turn affects the vapor flow field, this interaction requires the simultaneous consideration of the liquid and vapor layers.

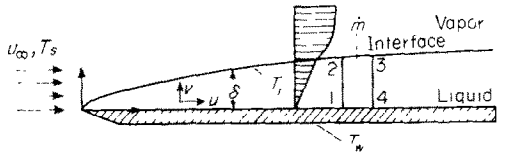

FIG. 1. Physical model and co-ordinates.

Governing equations

The basic governing partial differential equations and boundary conditions have been given in [5] and it is not necessary to repeat them here. By use of the Blasius-type similarity transformation, the partial differential equations can be transformed into a corresponding set of ordinary differential equations. The resulting transformed ordinary differential equations together with their boundary conditions are as follows.

Liquid film

$$f''' + \tfrac{1}{2}ff'' = 0 \tag{1}$$

$$\theta + \tfrac{1}{2}Prf\theta' = 0. \tag{2}$$

Vapor layer

$$F''' + \tfrac{1}{2}FF'' = 0. \tag{3}$$

Boundary conditions

$$\text{At } \eta_L = 0 \text{ (wall) } f = f' = 0 \quad \theta = 1 \tag{4}$$

$$\text{as } \eta_v \to \infty \text{ (vapor phase) } F' \to 1. \tag{5}$$

At the interface

$$\left.\begin{array}{l} \eta_L = \eta_\delta \\ \text{or} \\ \eta_v = 0 \end{array}\right\} \quad \begin{cases} \theta = 0 & (6) \\ F = Rf & (7) \\ F' = f' & (8) \\ F'' = Rf'' & (9) \end{cases}$$

where

$$' = \frac{\mathrm{d}}{\mathrm{d}\eta_L} \quad \text{or} \quad ' = \frac{\mathrm{d}}{\mathrm{d}\eta_v} \tag{10}$$

$$\eta_L = \frac{y}{x}\sqrt{\left(\frac{u_\infty x}{\nu_L}\right)}; \quad \eta_v = \frac{y}{x}\sqrt{\left(\frac{u_\infty x}{\nu_v}\right)} \tag{11}$$

$$f(\eta_L) = \frac{\psi_L}{\sqrt{(\nu_L u_\infty x)}}; \quad F(\eta_v) = \frac{\psi_v}{\sqrt{(\nu_v u_\infty x)}} \tag{12}$$

$$\theta(\eta_L) = \frac{T - T_s}{T_w - T_s} \tag{13}$$

$$R = \left[\frac{(\rho\mu)_L}{(\rho\mu)_v}\right]^{1/2} \tag{14}$$

$$u_L = \frac{\partial\psi_L}{\partial y} = u_\infty f'(\eta_L); \quad u_v = \frac{\partial\psi_v}{\partial y} = u_\infty F'(\eta_v) \tag{15}$$

$$\left.\begin{array}{l} v_L = -\dfrac{\partial\psi_L}{\partial x} = \tfrac{1}{2}\sqrt{\left(\dfrac{\nu_L u_\infty}{x}\right)}(\eta_L f' - f) \\ v_v = -\dfrac{\partial\psi_v}{\partial x} = \tfrac{1}{2}\sqrt{\left(\dfrac{\nu_v u_\infty}{x}\right)}(\eta_v F' - F). \end{array}\right\} \tag{16}$$

Notice that the above differential equations (1–3) together with the boundary conditions (4–9) involve three parameters Pr, $R = [(\rho\mu)_L/(\rho\mu)_v]^{1/2}$, and η_δ. From the energy balance at the interface, $-k_L\partial T/\partial y = \dot{m}h_{fg}$, it can be shown that the

dimensionless liquid-film thickness is implicitly related to the dimensionless physical group $c\rho\Delta T/Prh_{fg}$ by the following equation:

$$\frac{c_p\Delta T}{Prh_{fg}} = \frac{f(\eta_\delta)}{-2\theta'(\eta_\delta)}. \tag{17}$$

Hence, as soon as solutions are available as a function of η_δ, corresponding values of $c_p\Delta T/Prh_{fg}$ can be computed from equation (17). Consequently, the present problem in fact involves three physical parameters, Pr, R and $c_p\Delta T/Prh_{fg}$. It is interesting to note that the parameters involved are identical to those in film condensation in free convection [4]. Also in both cases, the parameters are similar to those in film boiling [7, 8].

Asymptotic expressions

Before we discuss the numerical solutions of the foregoing equations, it is worthwhile to consider two extreme cases, i.e. when the liquid film is either very thin or very thick.

(1) *Very thin liquid film.* When the liquid film is very thin, the liquid velocity is very small. Hence, the presence of the liquid film does not have any significant effect on the vapor boundary layer, and the vapor-velocity profile approaches to the Blasius profile. In this case, the vapor-velocity gradient at the interface is $F_i'' = 0{\cdot}332$, and the vapor velocity, velocity slope, temperature slope and the parameter $c_p\Delta T/Prh_{fg}$ can be written as follows:

$$f_\delta'' = \frac{F_i''}{R} = \frac{0{\cdot}332}{R} \tag{18}$$

$$f_\delta' = \frac{0{\cdot}332}{R}\eta_\delta \tag{19}$$

$$f_\delta = \frac{0{\cdot}166}{R}\eta_\delta^2 \tag{20}$$

$$\theta_\delta' = \theta_w' = -\frac{1}{\eta_\delta} \tag{21}$$

$$\frac{c_p\Delta T}{Prh_{fg}} R = \tfrac{1}{4} F_i''\eta_\delta^3 = 0{\cdot}083\,\eta_\delta^3. \tag{22}$$

A plot of $c_p\Delta T/Prh_{fg}$ vs. η_δ as calculated from equation (22) is shown in Fig. 4(c). When the liquid film is moderately thin, the velocity and temperature profiles are very close to straight lines. However, F_δ'' is now a function of the liquid film thickness η_δ. By following the treatment of [5], one can get a plot of $(c_p\Delta T/Prh_{fg})R$ vs. η_δ independent of R and Pr. Such a plot is also shown in Fig. 4(c) (see Results and Discussion).

(2) *Very thick liquid films.* When the liquid film is very thick (i.e. $\eta_\delta \to 7{\cdot}8$, [9]), the liquid–vapor interface velocity approaches to the free-stream velocity u_∞ and the liquid velocity profile would be essentially the same as the Blasius function. In this case, the following results are valid.

$$f''(\eta) = f_B''(\eta) \tag{23}$$

$$f'(\eta) = f_B'(\eta) \tag{24}$$

$$f(\eta) = f_B(\eta) \tag{25}$$

$$\frac{c_p\Delta T}{Prh_{fg}} = -\frac{f_B(\eta_\delta)}{2\theta_\delta'}. \tag{26}$$

Equation (26) indicates that $c_p\Delta T/Prh_{fg}$ is independent of R but a strong function of Pr (through θ_δ').

Methods of solutions

Before we discuss the method of solution it is helpful to point out that the momentum equations (1) and (3) are independent of the energy equation (2). Hence, for any pre-assigned value of η_δ and R, the momentum equations can be solved independently. Once this is done, the energy equation (2) can be readily integrated. The method used in solving the momentum equations (1) and (3) together with their boundary conditions, (4), (5) and (7–9) can be briefly described. For any given η_δ and R, a value of $f'(\eta_\delta)$ is guessed (remained to be checked). This guessed $f'(\eta_\delta)$ together with the boundary condition (4), $f(0) = f'(0) = 0$, allows us to solve the liquid momentum equation (1). The solution of equation (1) yields the values of f and f'' at the interface. The values of $F(0)$ and $F'(0)$ are then calculated from equations (7) and (8). These two conditions together with the boundary condition (5), $F'(\infty) = 1$ provide adequate boundary conditions for solving the vapor momentum equation (3). The solution of equations (3) yields among others the value of $F''(0)$. Now, since we

have the value of $F''(0)$ and the value of $f''(\eta_\delta)$, we can substitute them into equation (9). If equation (9) is satisfied, our guessed value for $f'(\eta_\delta)$ is correct and we have solved the momentum equations. Otherwise, a new value for $f'(\eta_\delta)$ must be used and the processes repeated until the final solution is obtained. With $f(\eta_\delta)$ available and Pr specified, the energy equation (2) together with its boundary conditions $\theta(0) = 1$ and $\theta(\infty) = 0$ can be solved by direct integration. This yields the temperature distribution across the liquid film. Finally, the value of the physical parameter $c_p\Delta T/Prh_{fg}$ corresponding to the prescribed η_δ is computed from equation (17).

Condensate flow rate, skin friction and heat transfer

Once the boundary-layer equations are solved, the values for $f''(0)$, $f(\eta_\delta)$ and $\theta(0)$ are available. The condensate flow rate, skin friction and heat transfer can then be computed by the following equations.

(1) *Condensation rate*

$$\left.\begin{aligned} &\textit{Dimensionless condensation rate}\\ &\frac{\dot{m}}{\rho_L u_\infty}\sqrt{(Re_x)} = \frac{f(\eta_\delta)}{2}\\ &\textit{Dimensionless liquid flow}\\ &\frac{\int_0^\delta \rho_L u\,\mathrm{d}y}{\rho_L u_\infty x}\sqrt{(Re_x)} = f(\eta_\delta) \end{aligned}\right\} \quad (27)$$

where $\dot{m}$ is the mass condensed per unit area per unit time while $\int_0^\delta \rho_L u\,\mathrm{d}y$ is the local mass flow of liquid in the direction parallel to the plates. From the relation $\bar{m}x = \int_0^\delta \rho_L u\,\mathrm{d}y$, it is evident that the average condensation rate $\bar{m}$ over a distance of x is equal to twice the local condensation rate $\dot{m}$, i.e.

$$\bar{m} = 2\dot{m}.$$

(2) *Skin friction*

$$\tfrac{1}{2}c_f\sqrt{(Re_x)} = f''(0) \quad (28)$$

where

$$c_f = \frac{\mu_L(\partial u/\partial y)_w}{\tfrac{1}{2}\rho_L u_\infty^2}. \quad (29)$$

(3) *Heat transfer*

$$\frac{Nu_x}{\sqrt{Re_x}} = -\theta'(0) \quad (30)$$

where

$$Nu_x = \frac{hx}{k} \quad (31)$$

$$h = \frac{q_w}{T_s - T_w}. \quad (32)$$

By integrating equation (30) with respect to x, it is found that the average heat transfer coefficient $\bar{h}$ is twice the local heat transfer coefficient, i.e.

$$\bar{h} = 2h. \quad (33)$$

RESULTS AND DISCUSSION

The two-phase condensation problem has been solved for three values of the $\rho\mu$ ratio ($R = 10$, 100, 500) and six values of the liquid Prandtl number ($Pr = 0{\cdot}003$, $0{\cdot}008$, $0{\cdot}03$, 1, 10, 100) with a wide range of liquid film thickness (and hence $c_p\Delta T/Prh_{fg}$). The results of solutions are presented in Figs. 2–8.

As mentioned in "Asymptotic expressions" in Section II, for very thin liquid film the vapor-velocity profile is essentially the same as the Blasius profile [9], and hence the vapor-velocity slope at the interface is practically a constant independent of the $\rho\mu$ ratio. Consequently, to satisfy the force balance at the interface, $[\mu(\partial u/\partial y)]_{L,i} = [\mu(\partial u/\partial y)]_{v,i}$, the slope of the liquid velocity must be a strong function of the $\rho\mu$ ratio. On the other hand, when the liquid film is very thick, the liquid-velocity profile is essentially the same as the Blasius profile, and in order to satisfy the force balance equation the vapor-velocity profile must be a strong function of the $\rho\mu$ ratio. Therefore, it can be realized that the $\rho\mu$ ratio would greatly influence the liquid-velocity distribution when the liquid film is relatively thin, and it would significantly affect the vapor-velocity profile when the liquid film is relatively thick. With this in mind, it is quite easy to understand the velocity profiles shown in Fig. 2(a) and (b). Fig. 2(a) indicates that the liquid velocity is essentially linear for $\eta_\delta = 1{\cdot}8$. However, their slopes depend strongly on the $\rho\mu$ ratio. The vapor-velocity profiles for the $\rho\mu$

ratio of 100 and 500 are somewhat different from each other. Nevertheless, for the scale used, they are essentially indistinguishable. For $\eta_\delta = 3{\cdot}5$, the liquid-velocity profile, as shown in Fig. 2(b), is nonlinear and is practically independent of the $\rho\mu$ ratio. Since the liquid film is relatively thick, the vapor-velocity profiles differ widely from each other for various $\rho\mu$ ratio.

The temperature profiles corresponding to $\eta_\delta = 1{\cdot}8$ are shown in Fig. 3. As expected, for liquids of low Prandtl number (liquid metals), the temperature profile is essentially linear. The nonlinearity increases with an increase of Prandtl number. This is due to the fact that the energy transfer by convection is more important for higher Prandtl number. The nonlinearity of temperature also increases with a decrease of the $\rho\mu$ ratio. This again is due to the higher convection current of the liquid at a lower $\rho\mu$ ratio. The temperature profiles for liquid metals ($Pr = 0{\cdot}003 \sim 0{\cdot}03$) with $\eta_\delta = 3{\cdot}5$ are essentially linear. For high Prandtl number, the value of $c_p\Delta T/Prh_{fg}$ corresponding to $\eta_\delta = 3{\cdot}5$ is out of the range of practical interest. Hence, to save space, the temperature profiles corresponding to $\eta_\delta = 3{\cdot}5$ are not shown in this paper.

Figures 4(a) and (b) show the relation between the liquid film thickness η_δ and the physical parameter $c_p\Delta T/Prh_{fg}$ for low and high Prandtl number respectively. It is seen that a thin liquid film (small η_δ) corresponds to a small value of

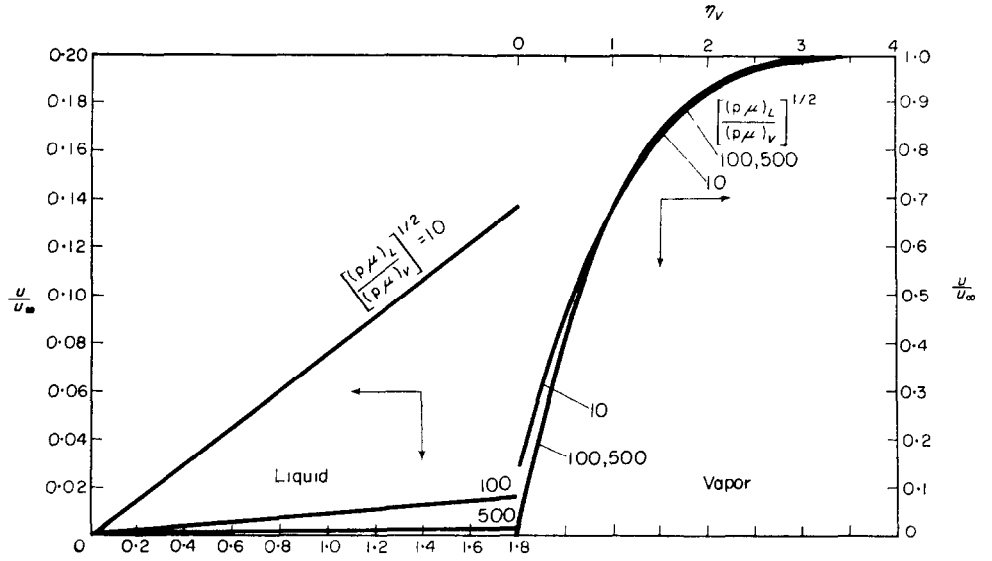

FIG. 2(a). Velocity profile $\eta_\delta = 1{\cdot}8$.

$\left[\frac{(\rho\mu)_L}{(\rho\mu)_v}\right]^{1/2}$	Pr	$\frac{c_v\Delta T}{h_{fg}Pr}$
10	0·003 ~ 0·008	0·1117
	0·03	0·1118
	1	0·1164
	10	0·1716
	100	19·63
100	0·003 ~ 0·03	0·01394
	1	0·01401
	10	0·01468
	100	0·02395
500	0·003 ~ 0·03	0·002880
	1	0·002883
	10	0·002911
	100	0·003208

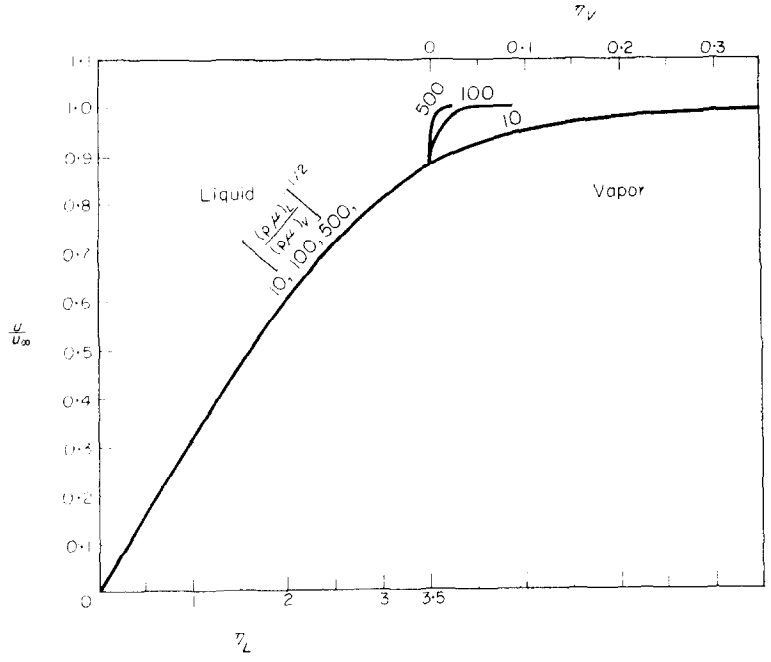

FIG. 2(b). Velocity profile $\eta_\delta = 3{\cdot}5$.

$\left[\frac{(\rho\mu)_L}{(\rho\mu)_v}\right]^{1/2}$	Pr	$\frac{C_p\Delta T}{h_{fg}\,Pr}$
10	0·003	3·078
	0·008	3·087
	0·03	3·126
100	0·003	3·072
	0·008	3·081
500	0·03	3·120

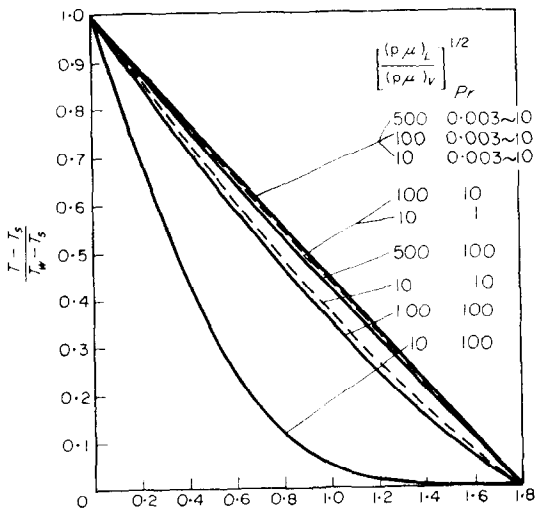

FIG. 3. Temperature profile, $\eta_\delta = 1{\cdot}8$.

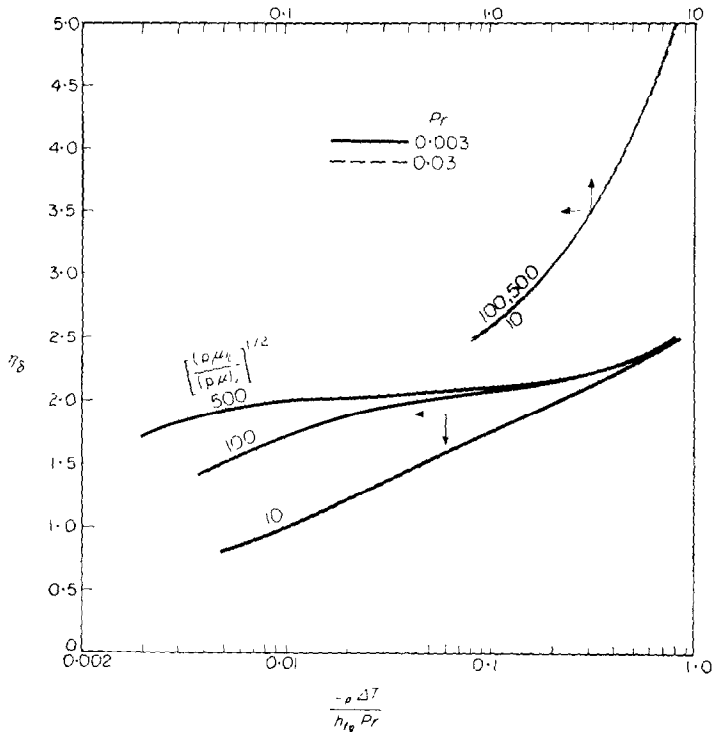

FIG. 4(a). Physical parameter, $c_p\Delta T/h_{fg}\,Pr$ and liquid film thickness η_δ (low Pr).

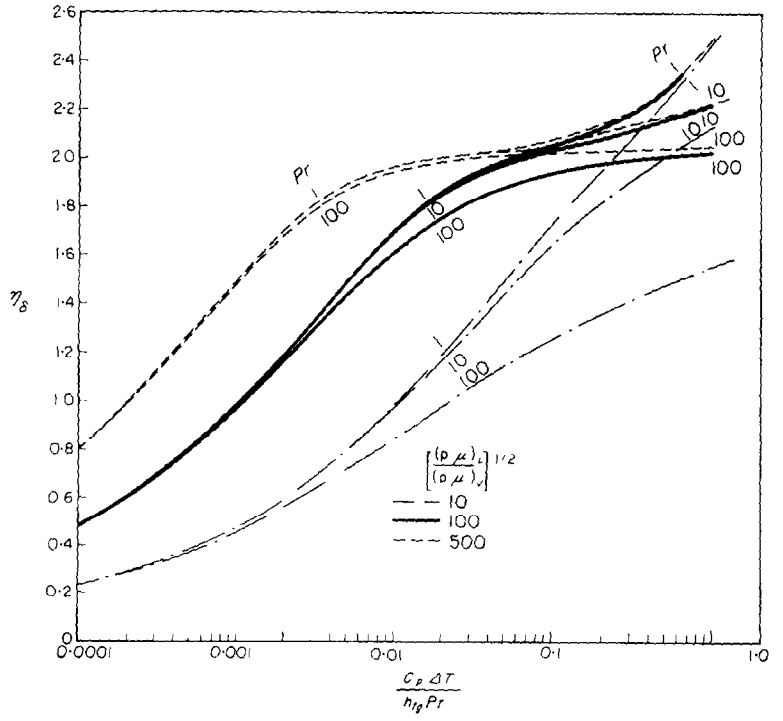

FIG. 4(b). Physical parameter, $c_p\Delta T/h_{fg}\,Pr$ and liquid film thickness η_δ (high Pr).

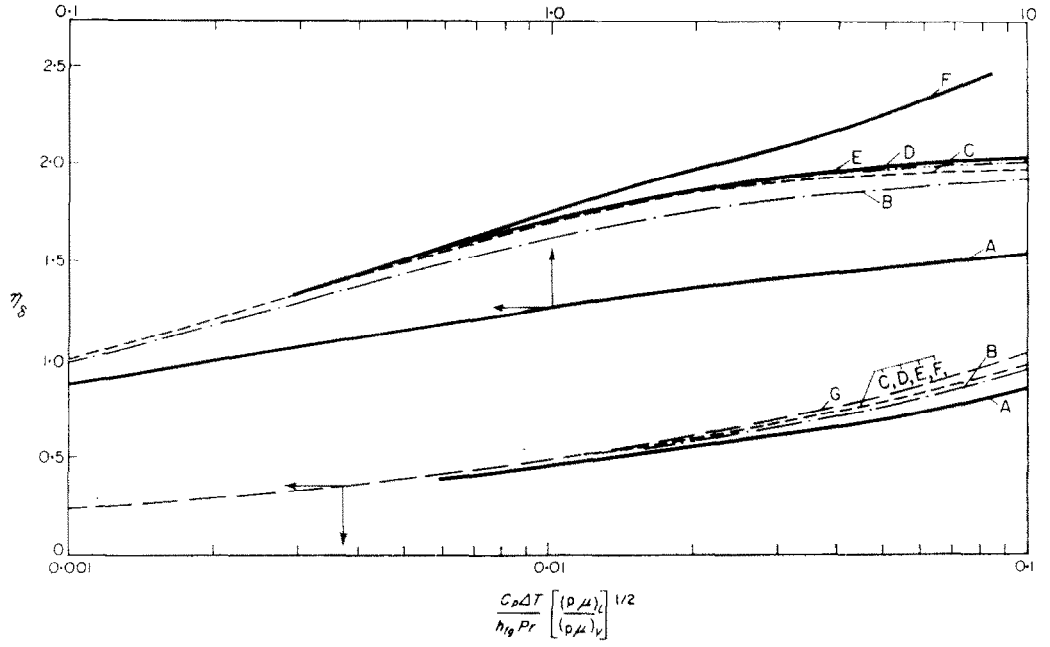

FIG. 4(c). $\frac{c_p \Delta T}{h_{fg} Pr}\left[\frac{(\rho\mu)_L}{\rho\mu)_v}\right]^{1/2}$ versus η_δ.

	Pr	$\left[\frac{(\rho\mu)_L}{(\rho\mu)_v}\right]^{1/2}$
A	100	10
B	100	100
C	(Cess [5])	
D	10	100
E	0·003 ~ 1	100
F	0·003 ~ 0·03	10
G	equation (22)	

$c_p \Delta T/Prh_{fg}$ and a thick liquid film corresponds to a large value of $c_p \Delta T/Prh_{fg}$. As shown in Fig. 4(a) for liquids of low Prandtl number, the relation between η_δ and $c\rho \Delta T/Prh_{fg}$ is essentially independent of the Prandtl number. This is because in liquids of low Prandtl number, the temperature profile for all Prandtl numbers is linear, and hence $c_p \Delta T/Prh_{fg}$ as calculated from equation (17) depends only on η_δ and the $\rho\mu$ ratio. Fig. 4(c) shows the relation between $c_p \Delta TR/Prh_{fg}$ and η_δ for $\eta_\delta < 2{\cdot}5$. The results based on equation (22) and Cess's analysis are also shown in the figure for comparison. It is seen from Fig. 4(c) that for very thin liquid films ($\eta_\delta < 0{\cdot}4$), equation (22) predicts the $c_p \Delta TR/Prh_{fg}$ correctly. For liquids of low Prandtl number with liquid-film thickness $\eta_\delta < 1{\cdot}5$, the functional relationship between $c_p \Delta TR/Prh_{fg}$ and η_δ can be accurately determined by Cess's analysis. The deviation between the present calculations and those of Cess increases as both η_δ and Pr increase. This is because the inertia forces and energy transfer by convection which were neglected in [5] become important.

Figure 5 shows the condensation rates and liquid flow as a function of the liquid-film thickness η_δ, with $\rho\mu$ ratio as parameter. The condensation rate (also liquid flow) approaches zero as the liquid-film thickness η_δ approaches zero. For very thick liquid film, the liquid-velocity profiles are essentially independent of the $\rho\mu$ ratio and hence the condensation flow rate is practically independent of the $\rho\mu$ parameter.

Figure 6 shows the dimensionless skin friction

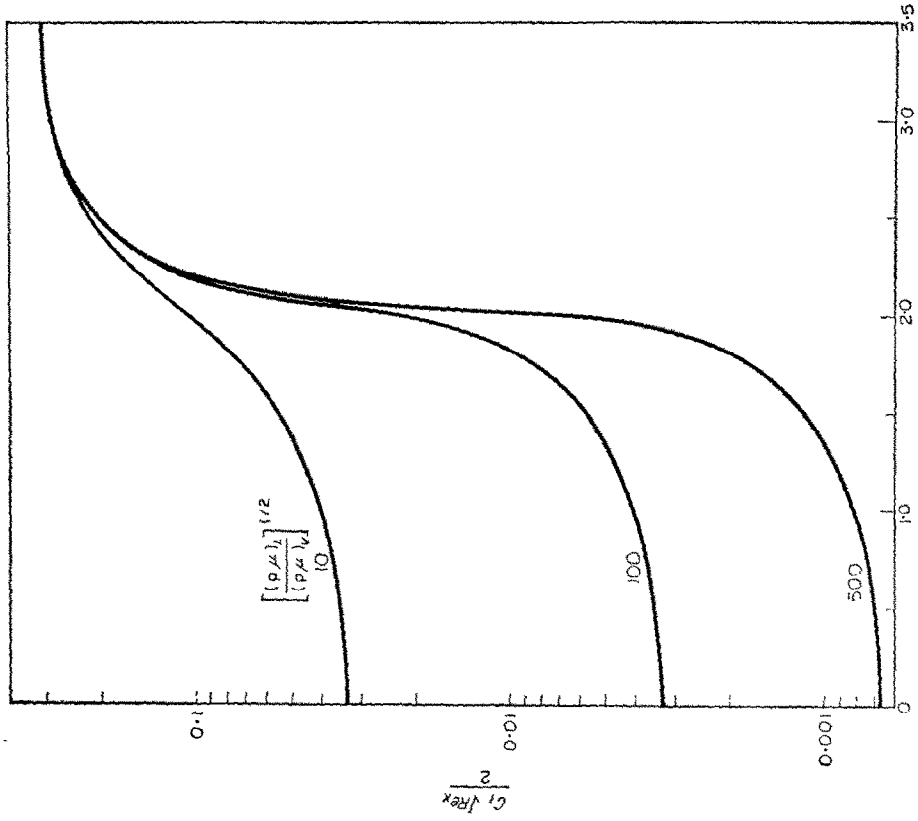

FIG. 6. Local skin friction.

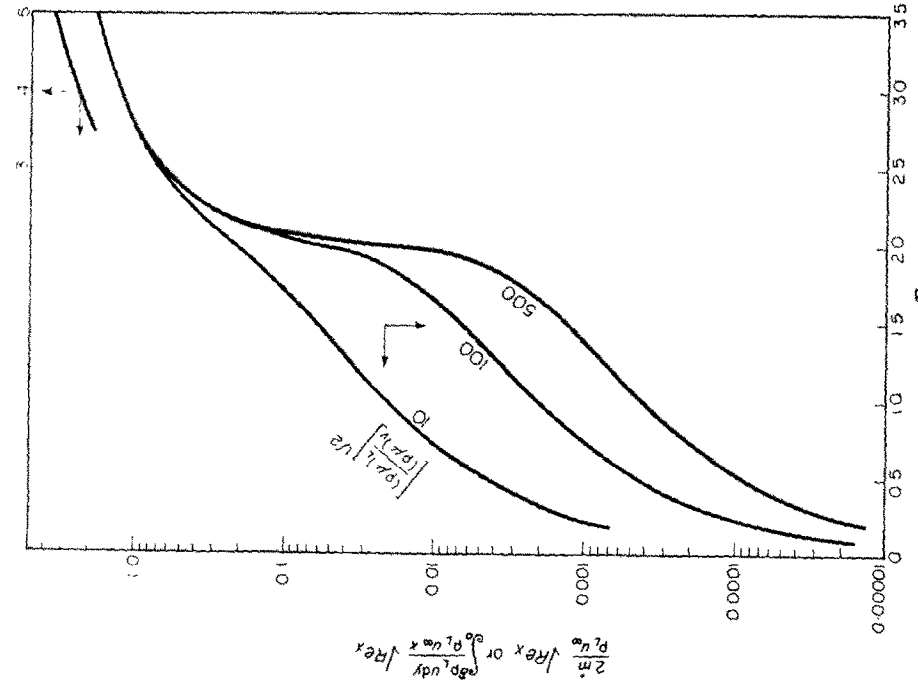

FIG. 5. Local condensation rates.

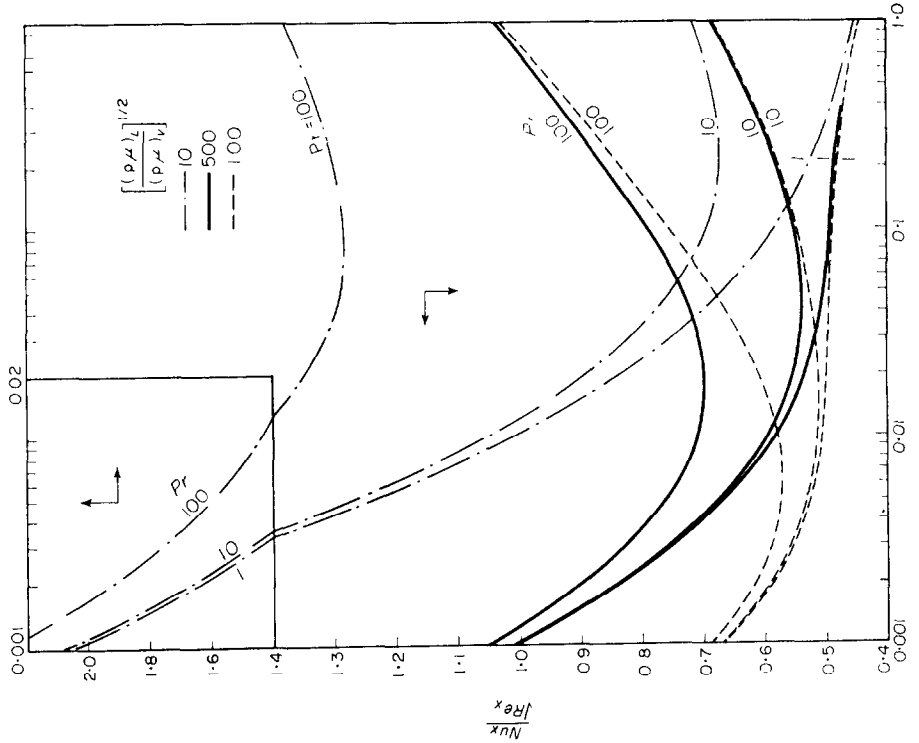

FIG. 7(b). Local heat transfer (high *Pr*).

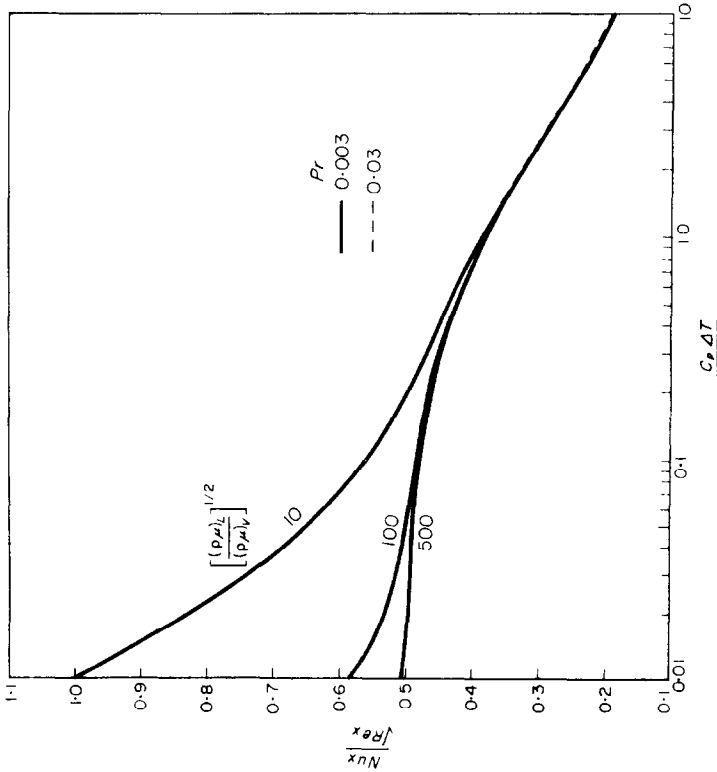

FIG. 7(a). Local heat transfer (low *Pr*).

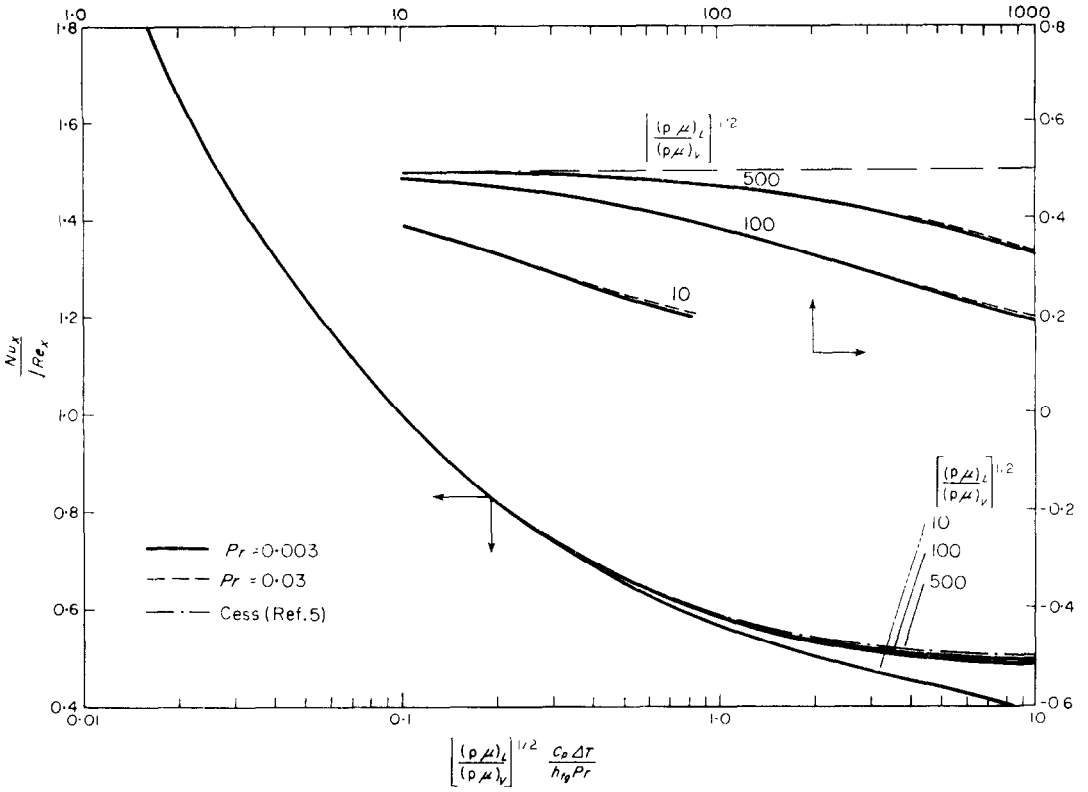

FIG. 8(a). Comparison of heat transfer between exact and approximate analysis (low Pr).

as a function of the liquid-film thickness. For very thin liquid film, the skin friction approaches the value corresponding to the case of no condensation [$f''(0)R = F''(0) = 0{\cdot}332$]. For very thick liquid layer, the skin friction approaches the value corresponding to the single-phase liquid flow [$f''(0) = 0{\cdot}332$].

Figures 7(a) and (b) show respectively the dimensionless heat transfer for low and high Prandtl number. It is seen from Fig. 7(a) that, for liquid metals (low Prandtl numbers), the dimensionless heat transfer is essentially independent of the Prandtl number and hence depends only on $c_p\Delta T/Prh_{fg}$ and R. This is because the temperature profiles are practically linear for all liquids of low Prandtl number (liquid metals) and hence the Prandtl number does not enter into the problem except in the dimensionless group $c_p\Delta T/Prh_{fg}$. For a fixed value of $Nu_x/\sqrt{Re_x}$ (or fixed η_δ since $Nu_x/\sqrt{(Re_x)} = \theta'(0) = 1/\eta_\delta$), Fig. 7(a) shows that $c_p\Delta T/Prh_{fg}$ decreases as the $\rho\mu$ ratio increases. This is due to the fact that the more viscous liquid (high $\rho\mu$ ratio) moves at a lower speed and hence, to satisfy the conservation of energy, equation (17), the value of $c_p\Delta T/Prh_{fg}$ must be smaller than that for less viscous liquid. Fig. 7(a) also shows that the heat transfer decreases monotonically as the liquid-film thickness increases. This is obvious since, in conduction heat transfer (liquid metals), the resistance to heat flow is proportional to the liquid-layer thickness. For high Prandtl number, Fig. 7(b) shows that the heat transfer is a strong function of Prandtl number especially when the liquid film is relatively thick. This is expected, since in this case the energy transfer by convection plays an important role. As shown in Fig. 7(b) the heat, transfer drops to a minimum value and then rises again as the liquid-film thickness increases.

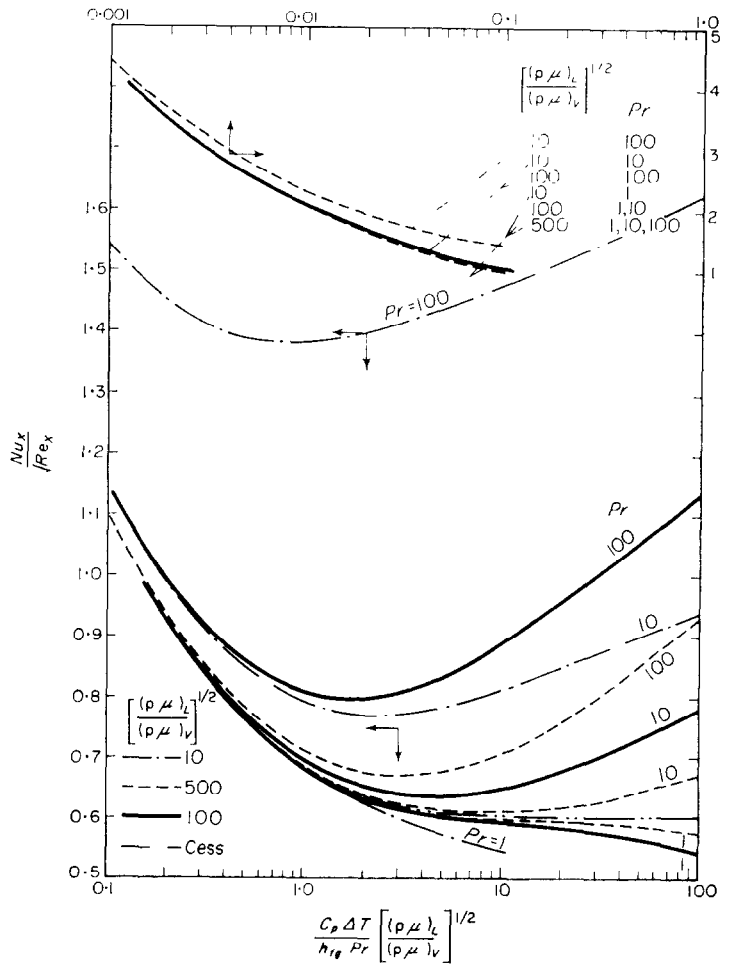

FIG. 8(b). Comparison of heat transfer between exact and approximate analyses (high *Pr*).

This can be explained by the fact that, as the film thickness increases, the energy transfer by conduction decreases while that by convection increases and consequently there exists a region where the dimensionless heat transfer reaches a minimum value. Figs. 4–8 furnish the complete information to compute the condensation rate, skin friction and heat transfer in laminar forced condensation on a flat plate. For any specified $c_p\Delta T/Prh_{fg}$, *Pr* and $\rho\mu$ ratio, one can determine the liquid-film thickness from Figs. 4(a), (b) and (c). The condensation rate, skin friction and heat transfer can then be read directly from Figs. 5, 6 and 7 or 8 respectively.

IV. COMPARISON OF RESULTS

Figures 8(a) and (b) show the comparison between the present calculations and the approximate solutions of Cess.* For liquid metals where the convection is not important, the heat-transfer results of Cess agree very well with the present calculation for small $RC_p\Delta T/Prh_{fg}$. The deviation increases as $Rc_p\Delta T/Prh_{fg}$ increases especially for small $\rho\mu$ ratio. For $Pr = 1$, Fig. 8(b) shows that the approximate

* The abscissa and ordinate used in Fig. 3 of [5] appear in different forms from those of Figs. 8(a) and (b) in this paper. Actually, they are identical with each other. Cess used ν_v while we use ν_L in *Re*.

treatment predicts the heat transfer quite well for almost the whole range of $Rc_p\Delta T/Prh_{fg}$. For higher Prandtl number, the approximate analysis underestimates the heat transfer considerably. This is because the energy transfer by convection is quite important for liquids of high Prandtl number, while it was neglected in Cess's analysis.

As mentioned in the Introduction, the same kind of problem was also treated in [6] by neglecting the vapor velocity at the liquid–vapor interface. Only two values of $c_p\Delta T/Prh_{fg}$ were calculated.

It was concluded in [6], that the solution does not depend on Pr explicitly and that the heat-transfer parameter $Nu_x/\sqrt{Re_x}$ decreases as $c_p\Delta T/Prh_{fg}$ increases. The present finding does not confirm these conclusions. As is evident from Figs. 7(a) and (b), the Prandtl number does not enter into the problem explicitly only for liquids of low Prandtl number (liquid metals). For liquids of high Prandtl number, solutions indeed depend on the Prandtl number. Also, $Nu_x/\sqrt{Re_x}$ decreases monotonically as $c_p\Delta T/Prh_{fg}$ increases only for liquids of low Prandtl number. For liquids of high Prandtl number, the heat-transfer parameter $Nu_x/\sqrt{Re_x}$ decreases to a minimum value and then rises again for the reason explained in Section III. We shall now use a numerical example (Table 1) to compare the heat-transfer results as calculated from different authors.

Table 1. Comparison of results

($Pr = 1$; $c_p\Delta T/Prh_{fg} = 0{\cdot}05$; $R = 200$)

η_δ	u_i/u_∞	$Nu_x/\sqrt{Re_x}$	Source
	0	0·53	(Chung, [6])
2·0	0·05	0·5	(Cess, [5])
2·05	0·07	0·495	(present calculation)

As can be seen from the table, the heat transfer as given in [6] for the specific example is too high by 7 per cent. Also, the results obtained from [5] agree well with the present calculations.

V. CONCLUSIONS

The two-phase boundary-layer equations in laminar film condensation for flow over a flat plate have been solved. The parameters involved are Pr, $[(\rho\mu)_L/(\rho\mu)_v]^{1/2}$ and $c_p\Delta T/Prh_{fg}$. It was found that, for liquids of low Prandtl number (liquid metals), the energy transfer by convection is negligibly small and hence only two parameters, $[(\rho\mu)_L/(\rho\mu)_v]^{1/2}$ and $c_p\Delta T/Prh_{fg}$ are important. In this case the heat transfer decreases monotonicly as $c_p\Delta T/Prh_{fg}$ (or liquid film thickness) increases. For high Prandtl number ($Pr > 1$) where the energy transfer by convection cannot be neglected, the dimensionless heat transfer, $Nu_x/\sqrt{Re_x}$, drops to a minimum value and then rises again as $c_p\Delta T/Prh_{fg}$ increases.

ACKNOWLEDGEMENT

The author wishes to express his appreciation to Mr. P. E. Grafton and Professor E. M. Sparrow for their many helpful discussions and suggestions, to Mr. J. Hughes for his help in computer programming, and to Mr. N. Carver for his preparation of figures.

REFERENCES

1. W. Nusselt, Die Obertachen Kondensation des Wasserdampfes. *Z. Ver. Dtsch. Ing.* **60**, 541, 569 (1916).
2. W. M. Rohsenow, Heat transfer and temperature distribution in laminar film condensation. *Trans. ASME*, **78**, 1645–1648 (1956).
3. E. M. Sparrow and J. L. Gregg, A boundary-layer treatment of laminar-film condensation. *Trans. ASME J. Heat Transfer*, C**81**, 13–18 (1959).
4. C. Y. Koh, E. M. Sparrow and J. P. Hartnett, The two-phase boundary layer in laminar-film condensation. *Int. J. Heat Mass Transfer*, **2**, 69–82 (1961).
5. R. D. Cess, Laminar-film condensation on a flat plate in the absence of a body force. *Z. Angew. Math. Phys.* **11**, 426–433 (1960).
6. P. M. Chung, Film condensation with and without body force in boundary-layer flow of vapor over a flat plate. *NASA* TN D-790 (1961).
7. R. D. Cess and E. M. Sparrow, Film boiling in a forced-convection boundary-layer flow. *Trans. ASME J. Heat Transfer*, C**83**, 370–376 (1961).
8. J. C. Y. Koh, Analysis of film boiling on vertical surfaces. *ASME* Pap. No. 61-SA-31, presented at the summer Annual Meeting, Los Angeles 1961; also to be published in *Trans. ASME J. Heat Transfer*.
9. H. Schlichting, *Boundary Layer Theory*. Pergamon Press, New York (1955).

Résumé—Cet article étudie la condensation par film laminaire d'un écoulement forcé de vapeur saturée sur une plaque plane. Le problème est formulé comme une solution exacte de couche limite. A partir des solutions numériques des équations fondamentales, on trouve que le transport d'énergie par convection est négigeable pour des liquides à bas nombre de Prandtl (métaux liquides) mais très important pour les liquides à nombre de Prandtl élevé. Le taux de condensation, le frottement à la paroi et la transmission de chaleur sont présentés graphiquement sous forme d'une fonction de $C_p\,\Delta T/Prh_{fg}$ ayant pour paramètre $[(\rho\mu)_L/(\rho\mu)_v]^{1/2}$ et Pr.

Zusammenfassung—Die laminare Filmkondensation von Sattdampf bei erzwungener Konvektion an einer ebenen Platte wird analysiert. Das Problem lässt sich als eine Exakte Grenzschichtlösung darstellen. Numerische Lösungen der massgeblichen Gleichungen zeigen, dass der Energieübergang durch Konvektion vernachlässigbar klein ist für Flüssigkeiten kleiner Prandtl-Zahl (flüssige Metalle) dagegen für solche grosser Prandtl-Zahlen sehr beachtlich wird. Kondensationsgeschwindigkeit, Oberflächenreibung und Wärmeübergang sind in Diagrammen als Funktion von $c_p\Delta T/Prh_{fg}$ mit $[(\rho\mu)_L/(\rho\mu)_v]^{1/2}$ und Pr als Parameter angegeben.

Аннотация—Рассматривается ламинарная плёночная конденсация из насыщенного пара при вынужденном течении на плоской пластине. Задача сформулирована как точное решение уравнений пограничного слоя. Путём численного решения основных уравнений найдено, что перенос энергии конвекцией пренебрежимо мал для жидкостей с низким числом Прандтля (жидкие металлы), но очень существенен для жидкостей с большим числом Прандтля. Скорость конденсации, поверхностное трение и теплообмен представлены графически как функция $c_p\Delta T/Prh_{fg}$ при параметрах $[(\rho\mu)_L/(\rho\mu)_v]^{1/2}$ и Pr.